Journal of Dental Research
2025, Vol. 104(6) 656–667

DOI: 10.1177/00220345241307944
journals.sagepub.com/home/jdr

Pericytes Are Odontoblast Progenitor Cells Depending on ER Stress

T. Ouchi[1], M. Ando[1], R. Kurashima[1], M. Kimura[1], N. Saito[2], A. Iwasaki[3], H. Sekiya[4], K. Nakajima[4], T. Hasegawa[1,5,6], T. Mizoguchi[7], and Y. Shibukawa[1]

Abstract

Odontoblasts are terminally differentiated cells that exhibit mechanosensitivity and mineralization capacity. Mechanosensitive ion channels such as Piezo1 are present in odontoblasts and are associated with their physiological functions via Ca^{2+} signaling. Both Ca^{2+} signals via Ca^{2+} influx from mechanosensitive ion channels and Ca^{2+} release from Ca^{2+} stores function as secondary messenger systems for various biological phenomena. The endoplasmic reticulum (ER) serves as an intracellular Ca^{2+} store that mobilizes intracellular Ca^{2+}. Changes in Ca^{2+} concentration inside the ER are among the factors that cause ER stress. Perivascular cells are located around odontoblasts in the dental pulp. Although such formation indicates that perivascular cells interact with odontoblasts, their detailed profiles under developmental and pathological conditions remain unclear. In this study, we revealed that pericyte marker, neural/glial antigen 2 (NG2)–positive cells, in cell-rich zones (CZs) can differentiate into Piezo1-positive odontoblasts following genetic odontoblast depletion in mice, and modeled as odontoblast death after severe dentin injury and as reparative dentin formation. NG2-positive pericytes differentiated into odontoblasts faster than glial cells. To determine how NG2-positive cells differentiate into Piezo1-positive odontoblasts, we focused on the ER-stress sensor protein, activating transcription factor 6a (ATF6a). After genetic odontoblast depletion, NG2-positive cells regenerated in the odontoblast layer and were capable of acting as functional odontoblasts. In the presence of extracellular Ca^{2+}, the application of a sarco/ER Ca^{2+}-ATPase (SERCA) inhibitor, thapsigargin, known as an ER-stress inducer, increased the intracellular Ca^{2+} concentration in the odontoblast lineage cells (OLCs). The increase was significantly inhibited by the application of a pharmacologic Piezo1 inhibitor, indicating that ER stress by SERCA inhibition augmented Piezo1-induced responses in odontoblast progenitor cells. However, the physiological activation of G_q-coupled receptors by adenosine diphosphate did not induce Piezo1 activation. Gene silencing of *ATF6a* and/or *NG2* impaired the mineralization of OLCs. Overall, ATF6a orchestrates the differentiation of NG2-positive pericytes into functional odontoblasts that act as sensory receptor cells and dentin-forming cells.

Keywords: NG2, ATF6a, dentin, dentinogenesis, ion channels, dental pulp

Highlights

- Pericytes located just beneath the odontoblast layer differentiate into functional odontoblasts.
- ATF6a regulates mechanosensitivity and dentin mineralization in odontoblasts.
- Pericytes are cell sources that contribute to odontoblast differentiation after odontoblast injuries.

Introduction

Odontoblasts are sensory receptor cells involved in sensory transduction, as an odontoblast hydrodynamic/mechanosensory receptor model (Shibukawa et al. 2015; Sato et al. 2018; Ohyama et al. 2022), and are essential for driving dentin mineralization (Goldberg and Smith 2004; Charadram et al. 2012; Neves and Sharpe 2018). Dentin mineralization is activated

Correction (March 2025): Article updated to correct figure 5X.

[1]Department of Physiology, Tokyo Dental College, Chiyoda-ku, Tokyo, Japan
[2]Department of Dental Anesthesiology, Tokyo Dental College, Chiyoda-ku, Tokyo, Japan
[3]Department of Oral Pathobiological Science and Surgery, Tokyo Dental College, Chiyoda-ku, Tokyo, Japan
[4]Department of Endodontics, Tokyo Dental College, Chiyoda-ku, Tokyo, Japan
[5]Department of Dentistry and Oral Surgery, Keio University School of Medicine, Shinjuku-ku, Tokyo, Japan
[6]Oral Surgery, Tokyo Metropolitan Cancer and Infectious Diseases Center, Komagome Hospital, Bunkyo-ku, Tokyo, Japan
[7]Oral Health Science Center, Tokyo Dental College, Chiyoda-ku, Tokyo, Japan

A supplemental appendix to this article is available online.

Corresponding Author:
Y. Shibukawa, Department of Physiology, Tokyo Dental College, 2-9-18, Kanda-Misaki-cho, Chiyoda-ku, Tokyo 101-0061, Japan.
Email: yshibuka@tdc.ac.jp

not only by physiological and developmental processes but also by mechanical, temperature-related, osmotic, and/or chemical stimulation to the dentin surface. In addition, dentin production by odontoblasts is a key process in developmental tooth formation, and understanding its detailed mechanism is important in generating drugs for dentin regeneration. Odontoblasts are well-polarized columnar cells that are aligned at the periphery of the dental pulp. To participate in dentin formation, they synthesize and secrete collagenous and noncollagenous matrix proteins as well as transcellular transportation of accumulated intracellular Ca^{2+} to the mineralizing front (Linde and Lundgren 1995). During dentinogenesis, transcellular Ca^{2+} transporting mechanisms are mediated by Ca^{2+} influx, mobilization, and extrusion (Linde and Lundgren 1995). These mechanisms include Ca^{2+} influx from the extracellular medium via various plasma membrane Ca^{2+} channels and Ca^{2+} release from intracellular inositol 1,4,5-trisphosphate (IP_3)- or ryanodine-sensitive Ca^{2+} stores (Lundgren and Linde 1997; Shibukawa and Suzuki 1997; Shibukawa and Suzuki 2003). An increased concentration of intracellular Ca^{2+} in odontoblasts is extruded by plasma membrane Na^{+}-Ca^{2+} exchanger (NCX) (Lundgren and Linde 1988; Tsumura et al. 2010) and plasma membrane Ca^{2+}-ATPase (PMCA) activity (Kimura et al. 2021).

Mouse incisors are model systems used to study the molecular mechanisms in the local niche environment and process of cell differentiation (Zhao et al. 2014). The neural/glial antigen 2 (NG2)–positive ($NG2^{+}$) pericytes display its position around vessels inside the odontoblast layer (OB) (Khatibi Shahidi et al. 2015). During steady state in the developmental process, odontoblasts originate from glial cells (Kaukua et al. 2014), while in injury repair for the dentin/pulp complex, odontoblasts are thought to originate from $NG2^{+}$ pericytes (Feng et al. 2011; Kaukua et al. 2014; Zhao et al. 2014). Single-cell RNA sequencing revealed that pericytes could be classified into 2 groups: positive for Nestin and NG2 ($Nestin^{+}$ $NG2^{+}$) and negative for Nestin and positive for NG2 ($Nestin^{-}$ $NG2^{+}$) (Gomes et al. 2022). Nestin is an odontoblastic marker protein (Nakatomi et al. 2018). When $NG2^{+}$ cells isolated from human dental pulp are treated with lipopolysaccharides, they exhibit stronger proliferation, migration, and odontoblastic differentiation, indicating their important role in rapid repair after injury of dentin/pulp complex (Yang et al. 2019). These results imply that $NG2^{+}$ pericytes are a potent candidate of cell source for odontoblast development.

Voltage-dependent L-type Ca^{2+} channels are expressed by $NG2^{+}$-pericyte lineage cells after dental pulp injury (Fu et al. 2023), while we have previously demonstrated that odontoblasts functionally express the mechanosensitive ion channel, Piezo1, and mechanical stimulation–induced intercellular Ca^{2+} signaling modulates mechanosensory transduction and mineralization of dentin (Matsunaga et al. 2021; Ohyama et al. 2022). Piezo1 channels in odontoblasts predominantly contribute to the detection of cellular deformation, as mechanical stimulation, induced by dentinal fluid movements in dentinal tubules during various stimuli applied to the exposed dentin surface. Activation of the Piezo1 channel and subsequent Ca^{2+} influx by Piezo1 negatively regulates reactionary dentinogenesis (Matsunaga et al. 2021). Owing to its essential properties, Piezo1 is useful odontoblast marker protein directly related to its cellular functions, dentin sensation, and dentinogenesis.

The endoplasmic reticulum (ER) serves as an intracellular Ca^{2+} store that releases and mobilizes intracellular Ca^{2+}. Factors that cause ER stress include changes and an imbalance in Ca^{2+} concentration inside the ER by releasing Ca^{2+} via IP_3 and/or ryanodine receptors from the store and by uptaking Ca^{2+} via sarco/ER Ca^{2+}-ATPase (SERCA) into the store (Ron and Walter 2007; Kim et al. 2008). The accumulation of unfolded proteins in the ER represents a cellular stress induced by multiple stimuli and pathological conditions. Although perivascular $NG2^{+}$ pericytes interact with odontoblasts for several reasons, their detailed developmental, physiological, and pathological profiles in association with the Ca^{2+} signals and subsequent ER stress remain unclear. Dental pulp is exposed to various stresses during the wound-healing process following dentin/pulp complex injury, and ER stress is assumed to occur via gene regulation of dental pulp cell properties (Walter and Ron 2011; Kim et al. 2014; Aryal et al. 2020; Li et al. 2022). Therefore, the purpose of this study was 2-fold. First, we elucidated the dynamic properties and characteristics of $NG2^{+}$ pericytes during functional odontoblast regeneration. Second, we examined the expression changes and regulatory mechanisms of ER-stress proteins during local differentiation of $NG2^{+}$ pericytes to odontoblasts.

Materials and Methods

The study was approved by our institute according to several guidelines described in the appendix. Other information is also described in the appendix.

Results

Expansion of $NG2^{+}$ Pericytes in Cell-Rich Zones after Odontoblast Death

To evaluate the microenvironment after odontoblast death, we administered diphtheria toxin (DT) every 24 h for 1 wk to *iDTR* and *Col1(2.3)Cre;iDTR* mice and sacrificed them on the eighth day (Fig. 1A). Morphological observations of the hematoxylin-eosin–stained dental pulp from *iDTR*- and *Col1(2.3)Cre;iDTR* mice incisors revealed highly polarized odontoblasts arranged at the dentin pulp border in *iDTR* mice (as a control) (OB; Fig. 1B1–B3) but not in *Col1(2.3)Cre;iDTR* mice (OB; Fig. 1C1–C3), enabling somatic odontoblast-specific depletion via DT administration. The expression of the odontoblast markers, Nestin and dentin sialophosphoprotein (DSPP), was observed in the OBs of *iDTR* mice (OB; Fig. 1D1–D3), but their levels were downregulated in *Col1(2.3)Cre;iDTR* mice (OB; Fig. 1E1–E3). The number of cells positive for Nestin and DSPP ($Nestin^{+}$ $DSPP^{+}$) in the OB was significantly lower in the odontoblast depletion model (*Col1(2.3)Cre;iDTR* mice) as compared with control (*iDTR* mice) (Fig. 1F). In wild-type

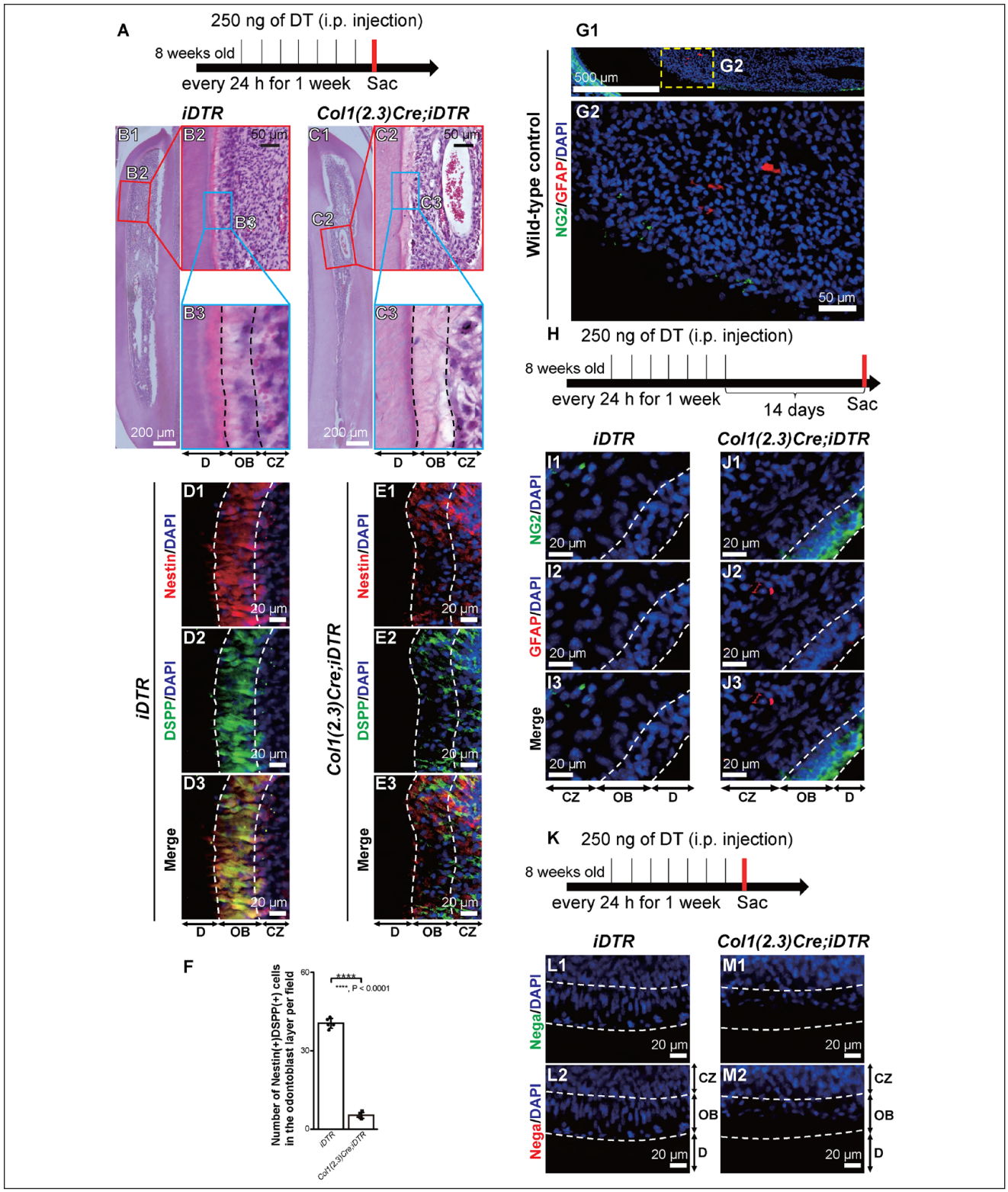

Figure 1. Cre recombination in *Col1(2.3)Cre;iDTR* mice drives odontoblast depletion. (**A**) Time course (arrow) of diphtheria toxin (DT; 250 ng) injection in both *iDTR* and *Col1(2.3)Cre;iDTR* mice. DT was injected intraperitoneally into 8-wk-old *iDTR* and *Col1(2.3)Cre;iDTR* mice for 7 consecutive days (vertical bars). The red vertical bar shows the time point of sacrificing (1 d after the last injection of DT). (**B1–C3**) Odontoblasts were depleted in the odontoblast layer (OB). Spindle-shaped cells were observed in the cell-rich zone (CZ) of the incisor in *Col1(2.3)Cre;iDTR* mice (C1–C3), whereas tall columnar odontoblasts were seen in *iDTR* mice incisor (B1–B3). Labels of D in (B3) and (C3) indicate dentin. (B2) Enlarged image of the inset of the red rectangle in (B1) for control *iDTR* mice. (B3) Enlarged image of the inset of the cyan rectangle in (B2) for control *iDTR* mice. (C2) Enlarged image of the inset of the red rectangle in (C1) for *Col1(2.3)Cre;iDTR* mice. (C3) Enlarged image of the inset of the cyan rectangle in (C2) for *Col1(2.3)Cre;iDTR*

mice. (**D1–E3**) Expression levels of the preodontoblast marker, Nestin, and mature odontoblast marker, DSPP, in control *iDTR* mice (D1–D3) were significantly downregulated in *Col1(2.3)Cre;iDTR* mice (E1–E3). Nuclei are shown in blue. (**F**) For the quantification of number of cells for Nestin and DSPP positive (Nestin$^+$ DSPP$^+$) in the OB in the *iDTR* and *Col1(2.3)Cre;iDTR* mice, Each bar represents the mean±standard deviation (SD) of each experiment (N=3 per group). A significant difference between columns (shown by solid line) is denoted by asterisks. The *P* value is shown (unpaired *t* test; parametric analysis). (**G1**, **G2**) Glial fibrillary acidic protein–positive (GFAP$^+$)–glial cells (red) were observed internally compared with neural/glial antigen 2–positive (NG2$^+$) pericytes (green) in dental pulp. (G2) Enlarged image of the inset of the dotted yellow rectangle in (G1). (**H–J3**) Time course (arrow) (H) of intraperitoneal DT administration (vertical bars) to 8-wk-old *iDTR* and *Col1(2.3)Cre;iDTR* mice for 7 consecutive days. Mice were sacrificed 14 d after the last injection (red vertical bar). (I1–J3) In *Col1(2.3)Cre;iDTR* mice, NG2$^+$ cells (green) were observed in the OB, whereas GFAP$^+$-glial cells (red) appeared late. Neither NG2$^+$ cells nor GFAP$^+$ glial cells were seen in OB in *iDTR* mice. Nuclei are shown in blue. (**K–M2**) Time course (arrow) (K) of intraperitoneal DT administration (vertical bars) to 8-wk-old *iDTR* and *Col1(2.3)Cre;iDTR* mice for 7 consecutive days. Mice were sacrificed 1 d after the last injection (red vertical bar). (L1–M2) Negative controls by omitting the first antibodies showed no immunoreactivities. Nuclei are shown in blue. i.p., intraperitoneal.

control mice (8 wk old), glial fibrillary acidic protein (GFAP)–positive (GFAP$^+$) glial cells were observed internally in the dental pulp of the incisors compared with where NG2$^+$ pericytes were observed (Fig. 1G1 and G2). When we observed mice for 14 d after the last injection of DT (Fig. 1H), NG2$^+$ cells were found to reach the OB earlier than GFAP$^+$-glial cells for their compensation as odontoblasts in *Col1(2.3)Cre;iDTR* mice incisors, indicating that NG2$^+$ pericytes, not glial cells, are local odontoblast progenitor cells (Fig. 1I1–J3). In the negative controls for immunofluorescence staining, we used samples short chased after odontoblast depletion models (Fig. 1K). The negative control by omitting the first antibodies showed no fluorescence detection (Fig. 1L1–M2). Thus, odontoblast depletion can trigger for NG2$^+$ pericytes migrating into the OB.

To identify the distribution patterns of pericytes, we conducted immunofluorescence staining using mandibular incisors. The number of NG2$^+$ cells was lower (Fig. 2A1, A2) than that of other pericyte markers such as platelet-derived growth factor receptor beta (PDGFRβ) (cluster of differentiation 140b; CD140b) (Fig. 2B1, B2), melanoma cell adhesion molecule (MCAM) (CD146) (Fig. 2C1, C2), and actin alpha 2 (Acta2) (alpha-smooth muscle actin; αSMA) (Fig. 2D1, D2). Due to the small number of NG2$^+$ pericytes in dental pulp, we hypothesized that they may exist as a minor population of stem cells or progenitor cells in dental pulp. Next, we performed immunofluorescence staining to determine how NG2$^+$ pericytes could differentiate into odontoblasts. Mandibular incisors were dissected from sacrificed mice after 7 consecutive days of DT administration (Fig. 2E). After DT administration, the number of NG2$^+$ pericytes increased in the cell-rich zone (CZ) and expressed Nestin (Fig. 2G1-H3), DSPP (Fig. 2K1-L3), and Piezo1 (Fig. 2O1-P3) in *Col1(2.3)Cre;iDTR* mice, while the small number of NG2$^+$ pericytes did not change obviously in *iDTR* mice (Fig. 2F1–F3, J1–J3, N1–N3). Cell shape of NG2$^+$ cells in CZ in *Col1(2.3)Cre;iDTR* mice showed several patterns due to the fact that pericytes are generally classified by their morphologies. In the CZ, the number of cells that were double-positive for NG2 and each odontoblast marker, Nestin, DSPP, and Piezo1, was dominant in *Col1(2.3)Cre;iDTR* mice compared with *iDTR* mice. The number of NG2$^+$ Nestin$^+$ cells in the CZ significantly increased by 7-fold in *Col1(2.3)Cre;iDTR* mice compared with *iDTR* mice (Fig. 2I). The number of NG2$^+$ DSPP$^+$ cells in the CZ also significantly increased by 6- to 7-fold in *Col1(2.3)Cre;iDTR* mice (Fig. 2M). NG2$^+$ Piezo1$^+$ cells in the CZ were dominant in *Col1(2.3)Cre;iDTR* mice (5-fold increase) relative to *iDTR* mice (Fig. 2Q).

Expression of ER-Stress Sensor Proteins after Odontoblast Death

We hypothesized that ER stress is involved in odontoblast differentiation under pathological conditions by odontoblast death (Fig. 3A). Antibodies against activating transcription factor 6a (ATF6a), inositol-requiring enzyme 1 α (IRE1a), and protein kinase RNA-like endoplasmic reticulum kinase (PERK), which are ER-stress sensor proteins, were used to evaluate their immunoreactivities. Piezo1-positive (Piezo1$^+$) odontoblasts expressed ATF6a and PERK but not IRE1a under physiological conditions in *iDTR* mice (Fig. 3B1–B3, E1–E3, H1–H3). In the CZ in *iDTR* mice, we observed the small number of ATF6a-positive (ATF6a$^+$) cells, IRE1a-positive (IRE1a$^+$) cells, and PERK-positive (PERK$^+$) cells. After odontoblast depletion mimicking dental pulp/odontoblast injury, ATF6a$^+$ Piezo1$^+$ cells were abundantly observed in the CZ (4- to 5-fold change) (Fig. 3C1–C3, D), whereas these changes could not be observed for IRE1a$^+$ Piezo1$^+$ cells and PERK$^+$ Piezo1$^+$ cells (Fig. 3F1–F3, G, I1–I3, J). These data indicate that ER-stress sensor proteins, especially ATF6a, may regulate the differentiation from pericytes into odontoblasts.

images of (L1) to (L3), respectively, indicating representative cells that were double-positive for both NG2 and DSPP (NG2$^+$ DSPP$^+$; pink-colored dotted lines) and cells that were single-positive for only NG2 (NG2$^+$ DSPP$^-$; cyan-colored dotted lines) in (L1) to (L3). Nuclei are shown in blue. (**M**) Increased number of NG2$^+$ DSPP$^+$ cells in *Col1(2.3)Cre;iDTR* mice incisors with a significant difference found compared with that in *iDTR* mice. (**N1–P3**) NG2$^+$ cells (green) were observed in the CZ and merged with the mechanosensitive ion channel, Piezo1 (red). Insets in (O1) to (O3) are shown as enlarged images of (P1) to (P3), respectively, indicating representative NG2$^+$ Piezo1$^+$ cells (P3). Nuclei are shown in blue. (**Q**) Increased number of NG2$^+$ Piezo1$^+$ cells in *Col1(2.3)Cre;iDTR* mice incisors with a significant difference found compared with that in *iDTR* mice. For the quantification of the number of NG2$^+$ Nestin$^+$ (I), NG2$^+$ DSPP$^+$ (M), and NG2$^+$ Piezo1$^+$ (Q) cells in the CZ, each bar represents the mean ± standard deviation of each experiment (*N* = 5 per group). Significant differences between columns (shown by solid lines) are denoted by asterisks. The *P* values are shown (unpaired *t* test; parametric analysis).

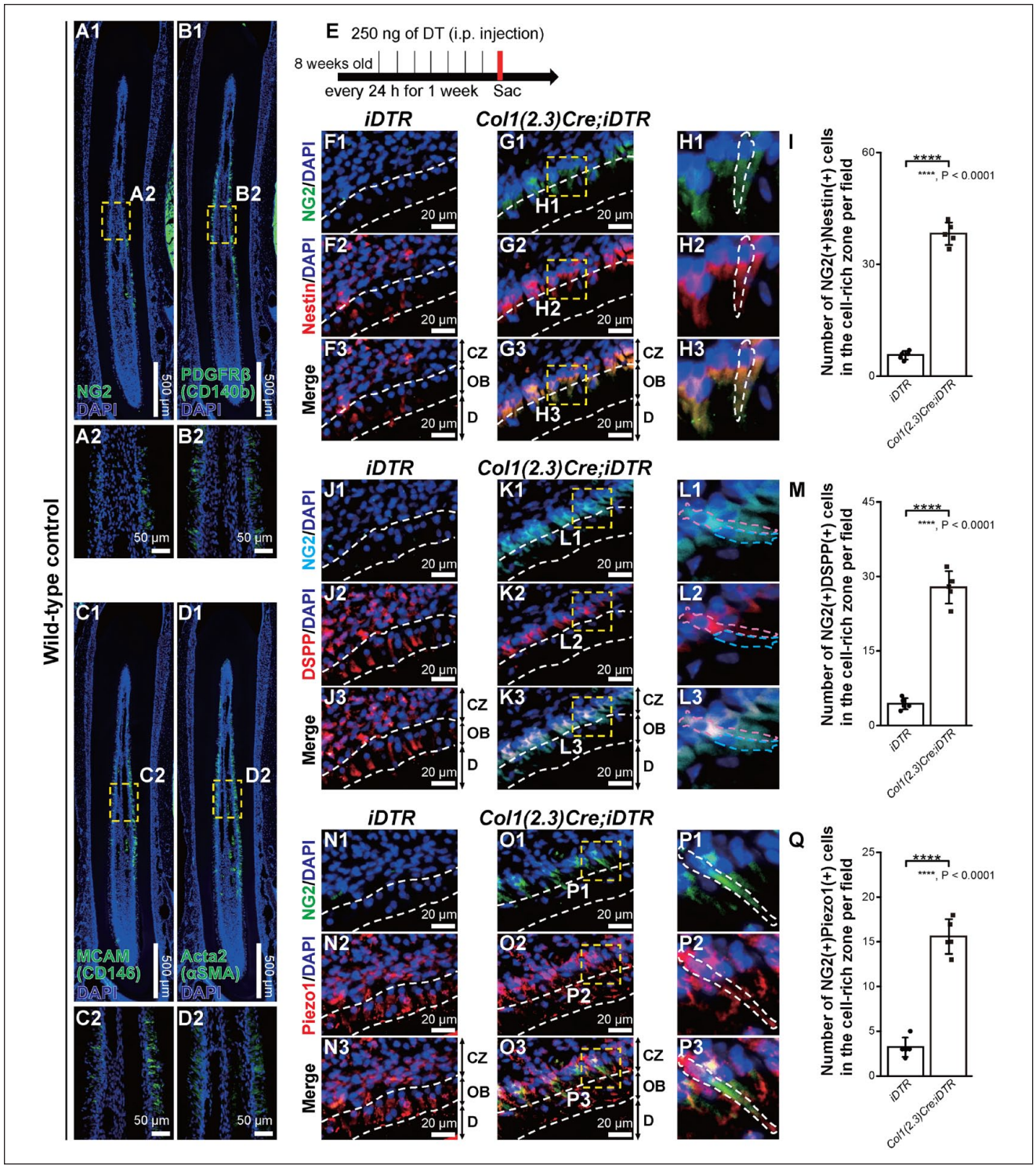

Figure 2. Expansion of neural/glial antigen 2–positive ($NG2^+$) cells in the cell-rich zone after odontoblast depletion. (**A1–D2**) Pericyte markers NG2 (A1 and A2), platelet-derived growth factor receptor beta (PDGFRβ) (CD140b) (B1 and B2), melanoma cell adhesion molecule (MCAM) (CD146) (C1 and C2), and Acta2 (alpha-smooth muscle actin; αSMA) (D1 and D2) were expressed in dental pulp. (**E**) Time course (arrow) of intraperitoneal diphtheria toxin (DT) administration to 8-wk-old *iDTR* and *Col1(2.3)Cre;iDTR* mice for consecutive 7 d (vertical bars). (**F1–H3**) $NG2^+$-cells (green) were observed in the cell-rich zone (CZ) and merged with the preodontoblast marker, Nestin (red), in *Col1(2.3)Cre;iDTR* mice (G1–G3), but not in *iDTR* mice (F1–F3). Insets in (G1) to (G3) are shown as enlarged images of (H1) to (H3), respectively, indicating representative $NG2^+$ $Nestin^+$ cells (H3). Nuclei are shown in blue. (**I**) Increased number of $NG2^+$ $Nestin^+$ cells in *Col1(2.3)Cre;iDTR* mice incisors with a significant difference found compared with that in *iDTR* mice. (**J1–L3**) $NG2^+$ cells (cyan) were observed in the CZ and merged with the mature odontoblast marker, dentin sialophosphoprotein (DSPP) (red), in *Col1(2.3)Cre;iDTR* mice (K1–K3) but not in *iDTR* mice (J1–J3). Insets in (K1) to (K3) are shown as enlarged

Differentiation of NG2⁺ Pericytes into Odontoblasts as Sensory Receptor Cells

To trace the differentiation of NG2⁺ pericytes into odontoblasts, we analyzed the *NG2CreERT2;tdTomato* mice. After tamoxifen was administered at postnatal day 3 of *NG2CreERT2;tdTomato* mice, incisor dental pulp cells were isolated and primary cultured in 1-mo-old mice (Appendix Fig. 1A). Cultured whole *NG2-tdTomato*–positive (*NG2-tdTomato*⁺) cells were immunopositive for Nestin (Appendix Fig. 1B1–B3), DSPP (Appendix Fig. 1C1–C3), Piezo1 (Appendix Fig. 1D1–D3), and runt-related transcription factor 2 (Runx2) (Appendix Fig. 1E1–E3). These results indicate that NG2⁺ pericytes have the potential to differentiate into odontoblast lineage cells.

Mouse incisors grow throughout their lives, whereas molars, like human teeth, have limited growth. Next, we used molar teeth and observed *Col1(2.3)Cre;iDTR* mice longer to see whether NG2⁺ cells in CZ differentiate into odontoblasts under the ATF6a regulatory mechanisms. We sacrificed *Col1(2.3)Cre;iDTR* mice 14 d after the last injection of DT (Fig. 4A). Regenerated NG2⁺ ATF6a⁺ cells after odontoblast death were located in the OBs of the molar tooth in *Col1(2.3)Cre;iDTR* mice (Fig. 4C1–C4), while NG2⁻ ATF6a⁺ cells were observed as steady state in OBs in *iDTR* mice (Fig. 4B1–B4). The number of NG2⁺ ATF6a⁺ cells in the CZ and the OB was significantly more dominant in *Col1(2.3)Cre;iDTR* mice than that in *iDTR* mice 14 d after odontoblast depletion (in CZ; 5-fold change/in OB; 4- to 5-fold change) (Fig. 4D, E). Because ATF6a activates by its nuclear translocation as an ER-stress response, we analyzed the ATF6a expression in nuclei in NG2⁻ ATF6a⁺ and NG2⁺ ATF6a⁺ cells. The data revealed greater observation of nuclear translocation of ATF6a in NG2⁺ cells than in NG2⁻ cells (3-fold change) (Fig. 4F, G).

Next, we analyzed nociceptive scores after application of cold water to exposed dentin in *iDTR* and *Col1(2.3)Cre;iDTR* mice. We chose 2 time points: (1) when odontoblasts were depleted (as day 1; 1 d after last DT administration) and (2) when pericyte-derived odontoblasts regenerated (as day 14; 14 d after last DT administration) (Fig. 4H). Nociceptive score data revealed that dentin mechanosensitivity of *Col1(2.3)Cre;iDTR* mice was recovered at the same level of *iDTR* mice, showing that NG2⁺ pericyte–derived odontoblasts gained a sensory receptor cell property (Fig. 4I). Immunofluorescent staining of regenerated odontoblasts, which were seen at 14 d after the last DT administration (Fig. 4J) in *Col1(2.3)Cre;iDTR* mice showed that they were immunopositive for Piezo1, similar to that in *iDTR* mice (Fig. 4K, N, N1). In addition, regenerated odontoblasts in *Col1(2.3)Cre;iDTR* mice expressed NCX1 and PMCA1, similar to that in *iDTR* mice (Fig. 4L, O, O1, M, P,

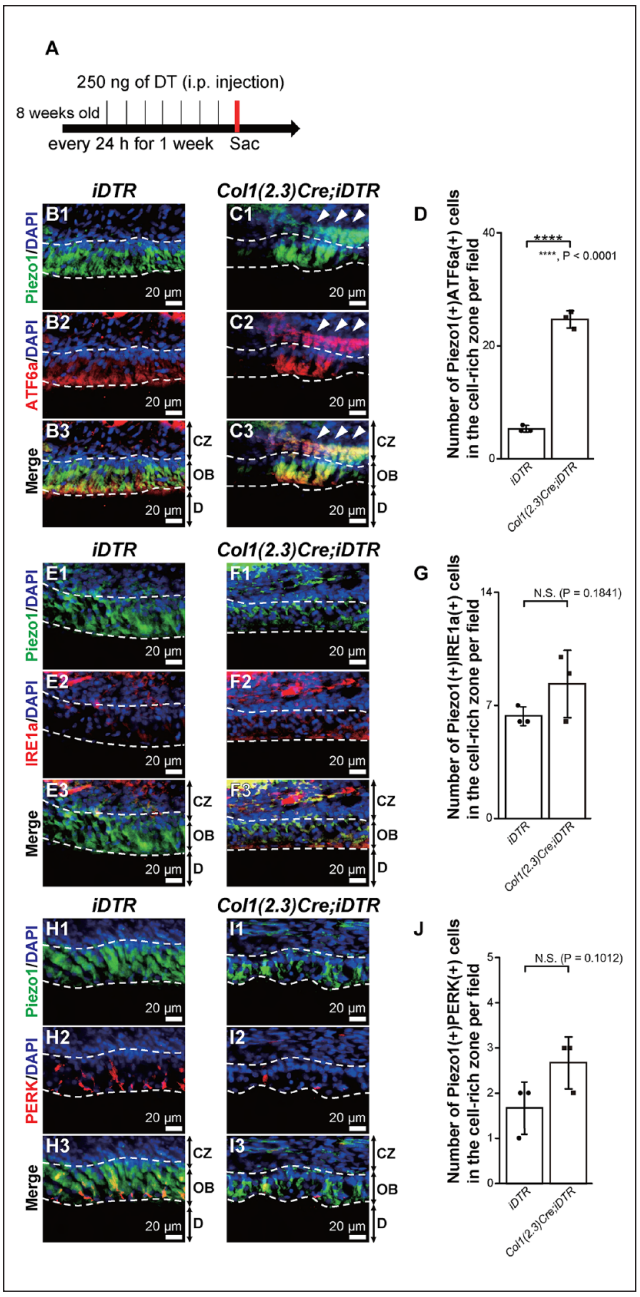

Figure 3. Expression of the endoplasmic reticulum stress marker, activating transcription factor 6a (ATF6a), in the cell-rich zone (CZ) after odontoblast depletion. (**A**) Time course (arrow) of intraperitoneal diphtheria toxin (DT) administration to 8-wk-old *iDTR* and *Col1(2.3)Cre;iDTR* mice for 7 consecutive days (vertical bars). (**B1–B3**) ATF6a (red) is expressed by Piezo1⁺ odontoblasts (green) in *iDTR* mice (as control). After odontoblast depletion in *Col1(2.3)Cre;iDTR* mice, Piezo1⁺ ATF6a⁺ cells were observed in the CZ (arrowheads in (**C1**) to (**C3**)). Nuclei are shown in blue. (**D**) A significantly greater number of Piezo1⁺ ATF6a⁺ cells was seen in *Col1(2.3)Cre;iDTR* mice compared with that in *iDTR* mice. (**E1–F3** and **H1–I3**) Slight but nonsignificant increase in the number of Piezo1⁺ cells (green) positive for other ER-stress markers, inositol-requiring enzyme 1 α (IRE1a) (red in E2, E3, F2, and F3) and protein kinase RNA-like endoplasmic reticulum kinase (PERK) (red in H2, H3, I2, and I3), was seen in the CZ in *Col1(2.3)Cre;iDTR* mice compared with that in *iDTR* mice. Nuclei are shown in blue. For the quantification of the number of Piezo1⁺ ATF6a⁺ (D), Piezo1⁺ IRE1a⁺ (**G**), and Piezo1⁺ PERK⁺ (**J**) cells in the CZ, each bar represents the mean ± standard deviation of each experiment ($N = 3$ per group). A significant difference between columns (shown by solid line) is denoted by asterisks. Nonsignificant differences are shown as N.S. The *P* values are shown (unpaired *t* test; parametric analysis).

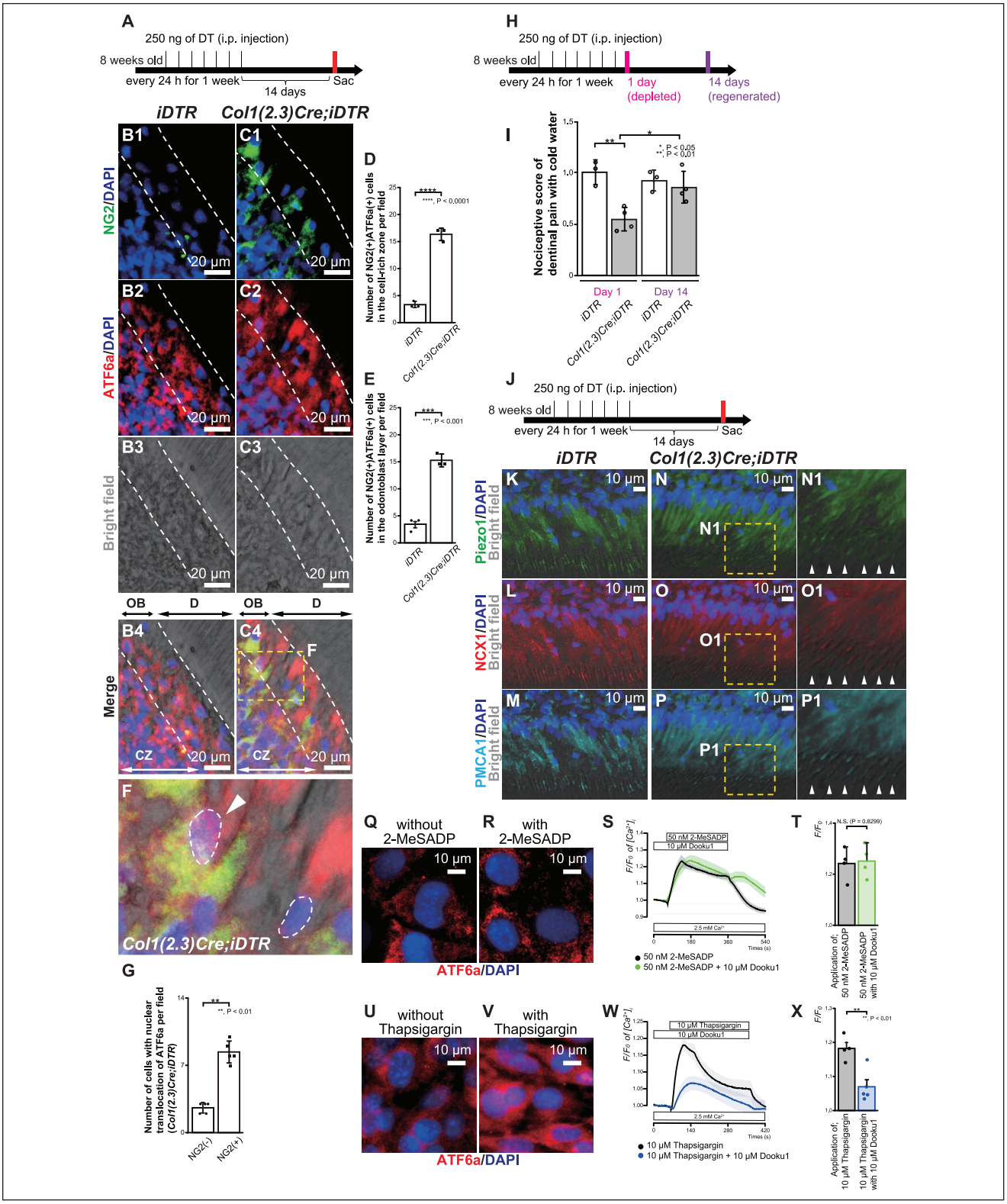

Figure 4. Neural/glial antigen 2–positive (NG2$^+$) pericyte–derived odontoblasts exhibited a sensory receptor cell property. (**A**) Time course (arrow) of intraperitoneal diphtheria toxin (DT) injection (vertical bars) into 8-wk-old *iDTR* and *Col1(2.3)Cre;iDTR* mice for 7 consecutive days. Sacrificing and sample harvesting (red bar) were conducted 14 d after the last injection of DT. (**B1–C4)** Fourteen days allowed the migration of NG2 (green)$^+$ activating transcription factor 6a (ATF6a) (red)$^+$ cells into the odontoblast layer in *Col1(2.3)Cre;iDTR* mice molars, whereas NG2$^+$ cells could not be seen in the odontoblast layer in *iDTR* mice. Nuclei are shown in blue. (**D and E**) An increased number of NG2$^+$ ATF6a$^+$ cells with significant

differences in both locations of the cell-rich zone (CZ) (D) and odontoblast layer (OB) (E) was observed in *Col1(2.3)Cre;iDTR* mice compared with that in *iDTR* mice; each bar represents the mean ± standard deviation (SD) of each experiment ($N = 3$ per group). Significant differences between columns (shown by solid lines) are denoted by asterisks. The *P* values are shown (unpaired *t* test, parametric analysis). (**F**) Nuclear translocation of ATF6a was observed in $NG2^+$ cells in *Col1(2.3)Cre;iDTR* mice (arrowhead). The image in (F) indicates the inset from the dotted yellow rectangle in (C4). Nuclei are shown in blue. (**G**) A significant increase in the number of cells with nuclear translocation of ATF6a in $NG2^+$ cells was observed compared with that in $NG2^-$ cells; each bar represents the mean ± SD of each experiment ($N = 5$ per group). A significant difference between columns (shown by solid line) is denoted by asterisks. The *P* value is shown (Kolmogorov–Smirnov nonparametric test). (**H**) Time course (arrow) of intraperitoneal DT injection (vertical bars) into 8-wk-old *iDTR* and *Col1(2.3)Cre;iDTR* mice for 7 consecutive days. The first demonstrations of the behavioral test (pink bar) were conducted 1 d after the last injection of DT. The second demonstrations of the behavioral test (purple bar) were conducted 14 d after the last injection of DT. (**I**) A significant decrease in nociceptive score was observed in *Col1(2.3)Cre;iDTR* mice ($N = 4$) after odontoblast depletion compared with those from *iDTR* mice ($N = 3$), and the decreases in the nociceptive score in *Col1(2.3)Cre;iDTR* mice were recovered at the same level of those measured in *iDTR* mice at 14 d after the last injection of DT. There was no significant difference in the score from *iDTR* mice measured between day 1 and day 14. (**J**) Time course (arrow) of intraperitoneal DT injection (vertical bars) into 8-wk-old *iDTR* and *Col1(2.3)Cre;iDTR* mice for 7 consecutive days. Sacrificing and sample harvesting (red bar) were conducted 14 d after the last injection of DT. (**K–P1**) Regenerated odontoblasts were immunopositive for the mechanosensitive ion channel, Piezo1 (green in K, N, and N1). Regenerated odontoblasts were also immunopositive for NCX1 (red in L, O, and O1) and plasma membrane Ca^{2+}-ATPase 1 (PMCA1; cyan in M, P, and P1); both are essential proteins for Ca^{2+} extrusion. (**Q, R**) ATF6a expression was observed in intracellular space but not in the nuclear location after application of 50 nM 2-MeSADP. (**S**) The effect of 10 μM Dooku1, a pharmacologic Piezo1 inhibitor, on 2-MeSADP (50 nM)–induced $[Ca^{2+}]_i$ increase was analyzed in odontoblast lineage cells (OLCs). 2-MeSADP activates $P2Y_1R$, known as a phospholipase C (PLC)–coupled G_q-protein coupled receptor, and induces Ca^{2+} release from the endoplasmic reticulum (ER). In the presence of extracellular Ca^{2+} (2.5 mM), a 5-min application of 50 nM 2-MeSADP increased $[Ca^{2+}]_i$ to the peak value of 1.24 ± 0.03 in F/F_0 units ($N = 4$). The increase was not inhibited by the application of 10 μM Dooku1 to the peak value of 1.25 ± 0.03 ($N = 4$), indicating that Ca^{2+} release from the ER via activation of the G_q-protein coupled receptor did not induce the augmentation of the Piezo1-induced response in OLC. Averaged traces of transient $[Ca^{2+}]_i$ increase in response to 50 nM 2-MeSADP in standard extracellular solution are shown. (**T**) The summary bar graphs representing values of F/F_0 for the increases in $[Ca^{2+}]_i$ by 50 nM 2-MeSADP (gray column) or 50 nM 2-MeSADP with 10 μM Dooku1 (green column). Note that odontoblast death can release adenosine triphosphate (ATP) to the surrounding tissue. Released ATP is immediately hydrolyzed by nucleoside triphosphate diphosphohydrolase-2 to produce adenosine diphosphate (ADP). These results suggest that even though ADP activates $P2Y_1R$ in the OLCs and Ca^{2+} release from ER follows, this physiological response by ADP does not induce ER stress. (**U, V**) ATF6a was nuclear translocated after application of 10 μM thapsigargin. (**W**) The effect of 10 μM Dooku1 on the thapsigargin (10 μM)–induced $[Ca^{2+}]_i$ increase was analyzed in OLCs. Thapsigargin suppressed sarco/ER Ca^{2+}-ATPase (SERCA) in the ER as Ca^{2+} stores and evoked a transient $[Ca^{2+}]_i$ increase by Ca^{2+} releasing from the stores. In the presence of extracellular Ca^{2+} (2.5 mM), a 5-min application of 10 μM thapsigargin increased $[Ca^{2+}]_i$ to the peak value of 1.18 ± 0.02 in F/F_0 units ($N = 4$). The increase was significantly inhibited by the application of 10 μM Dooku1 to the peak value of 1.06 ± 0.02 in F/F_0 units ($N = 5$), indicating that ER stress by SERCA inhibition augmented Piezo1-induced responses in OLCs. Averaged traces of a transient $[Ca^{2+}]_i$ increase in response to 10 μM thapsigargin in standard extracellular solution are shown. (**X**) Summary bar graphs representing values of F/F_0 for the increases in $[Ca^{2+}]_i$ by 10 μM thapsigargin (gray column) or 10 μM thapsigargin with 10 μM Dooku1 (blue column). (S, W) The boxes indicate the timings at which the test solutions (white boxes at the top) were applied. (T, X) The resting value is defined as $F/F_0 = 1.0$. Each bar indicates the mean ± standard error. A significant difference between columns (shown by solid line) is denoted by asterisks. A nonsignificant difference is shown as N.S. The *P* values are shown (unpaired *t* test; parametric analysis).

P1), both of which have essential roles in maintaining Ca^{2+} homeostasis.

Change and imbalance of the internal ER Ca^{2+} concentration ($[Ca^{2+}]_{ER}$) and intracellular Ca^{2+} concentration ($[Ca^{2+}]_i$) can induce ER stress. We next measured $[Ca^{2+}]_i$ by applying 2-methylthio-ADP (2-MeSADP; an agonist of $P2Y_{1, 12, 13}$ receptors) and the ER-stress inducer thapsigargin (a potent and noncompetitive inhibitor of SERCA) in mouse odontoblast lineage cells (OLCs). OLCs expressed Nestin, DSPP, and Piezo1 (Appendix Fig. 2A–C). OLCs were also immunopositive for $P2Y_1$ receptor ($P2Y_1R$) as well as Gnaq, which encodes the heterotrimeric G-protein α-subunit $G\alpha_q$ (Appendix Fig. 2D–F). Data showed that 1-h application of 10 μM thapsigargin (Fig. 4U, V) but not 50 nM 2-MeSADP (Fig. 4Q, R) induced nuclear translocation of ATF6a, confirming that the ER-stress response was induced by pathological SERCA regulation. Furthermore, we examined the effect of 10 μM Dooku1, a pharmacologic Piezo1 inhibitor, on 50 nM 2-MeSADP– or 10 μM thapsigargin-induced $[Ca^{2+}]_i$ increases in OLCs. In the presence of extracellular Ca^{2+} (2.5 mM), a 5-min application of 2-MeSADP or thapsigargin increased $[Ca^{2+}]_i$ in OLCs. The application of Dooku1 significantly inhibited the increase of $[Ca^{2+}]_i$ by thapsigargin but not the increase of $[Ca^{2+}]_i$ by 2-MeSADP, indicating that ER stress by SERCA inhibition augmented Piezo1-induced responses in OLCs (Fig. 4S, T, W, X).

Thus, we qualified $NG2^+$ pericyte–derived odontoblasts functioning as sensory receptor cells via Piezo1. To further determine the function of regenerated odontoblasts, we next investigated the dentin mineralization ability of $NG2^+$ pericyte–derived odontoblasts in molar teeth.

ATF6a, a Key Driver of Dentinogenesis Driven by $NG2^+$ Pericytes

We analyzed whether $NG2^+$ pericytes are cell sources for odontoblasts in molars in physiological condition. We produced genetically NG2 reporter mice (*NG2CreERT2;tdTomato* mice) and traced $NG2^+$ pericytes and their descendants. One day after tamoxifen injection (Fig. 5A), *NG2-tdTomato*–positive (*NG2-tdTomato*$^+$) cells, expressing the other pericyte marker PDGFRβ and the preodontoblast marker Nestin, were located around blood vessels (Fig. 5B1–B6). Fourteen days after tamoxifen injection (Fig. 5C), *NG2-tdTomato*$^+$ cells were located around the odontoblast niche in the molar (Fig. 5D1–E4). In addition, in different mammal species, NG2 was expressed in cells during odontoblast differentiation (Fig. 5F, G). These data indicate that $NG2^+$ pericytes are local cell sources for odontoblasts.

We further examined whether mechanical injury to the molar dentin can induce regenerative dentinogenesis via

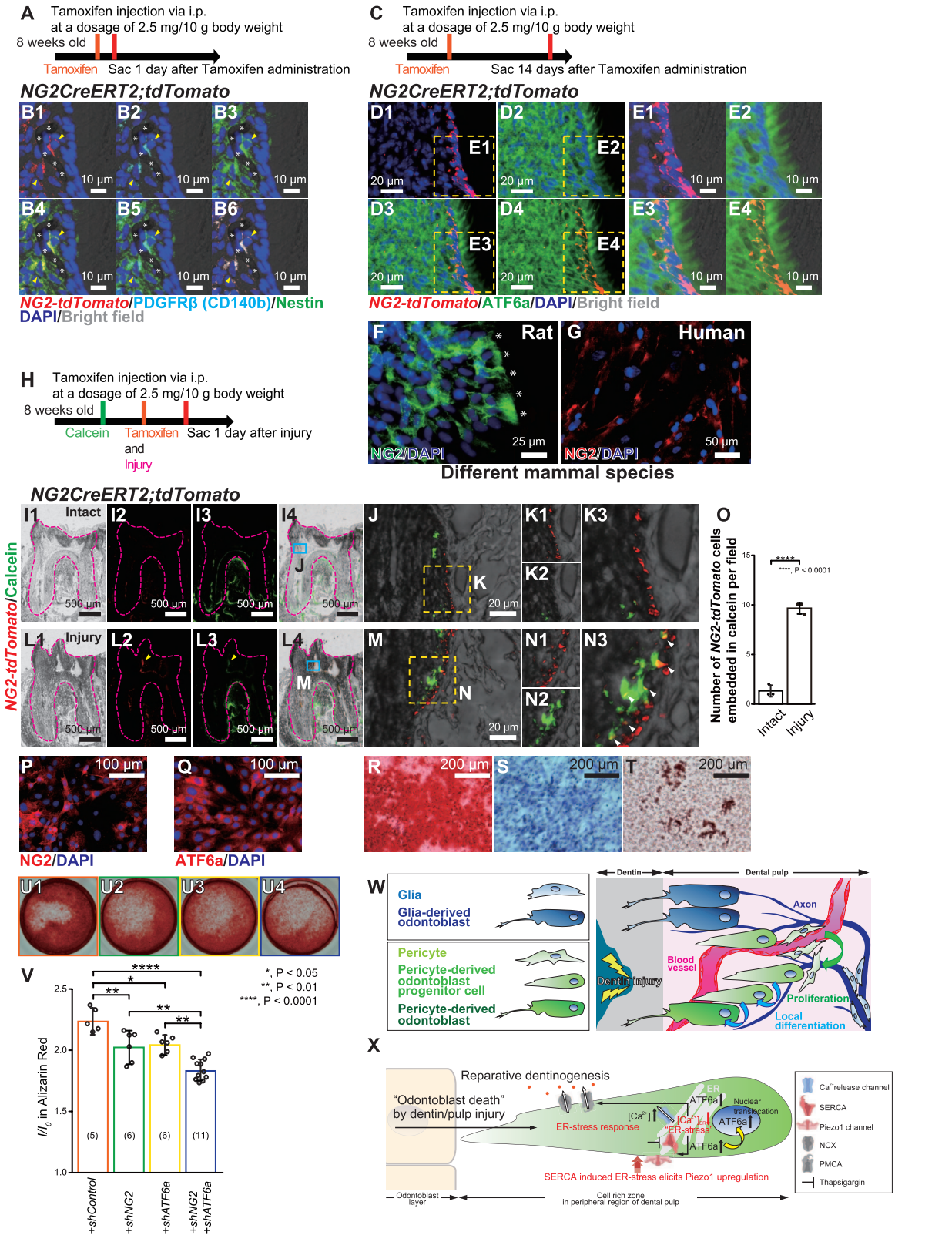

Figure 5. Activating transcription factor 6a (ATF6a) regulates the mineralization driven by neural/glial antigen 2–positive (NG2$^+$) pericytes. **(A–B6)** Time course (arrow) (A) of tamoxifen injection into 8-wk-old *NG2CreERT2;tdTomato* mice. Mice were sacrificed 1 d after tamoxifen administration. (B1–B6) Molar tooth showing that the NG2$^+$ pericytes and their descendants (red) are located nearby blood vessels (indicated by asterisks).

NG2$^+$ pericytes and their descendants (red) were also immunopositive for the other pericyte marker platelet-derived growth factor receptor beta (PDGFRβ; cyan) and preodontoblast marker Nestin (green) in *NG2CreERT2;tdTomato* mice (indicated by yellow arrowheads). (**C–E4)** Mice were sacrificed 14 d after tamoxifen administration. (D1–D4) Molar tooth showing the dominant expression of ATF6a (green) in molar dental pulp in *NG2CreERT2;tdTomato* mice. NG2$^+$ pericytes and their descendants are shown in red. Insets showing the dotted yellow rectangles in (D1) to (D4) were enlarged as images in (E1) to (E4), respectively. (**F**) A part of the rat odontoblasts (indicated by asterisks) in the dental pulp slice were immunopositive for NG2 antibody. (**G)** Human dental pulp cells with odontoblastic differentiation showed immunopositivity for NG2 antibody. Nuclei are shown in blue. (**H–N3**) Time course (arrow) (H) of calcein (green vertical bar) and both tamoxifen administration and injury (orange vertical bar) to 8-wk-old *NG2CreERT2;tdTomato* mice. Calcein was injected intraperitoneally (i.p.) 1 d before applying injury to the molars. Tamoxifen was then injected on the day of injury. Mice were sacrificed 1 d after injury (red vertical bar). **(I1–N3)** The dotted pink lines indicate the tooth morphology. The green color shows calcein, indicating the mineralizing front in molar subjected to injury (L1–L4) and that not subjected to injury (I1–I4). Insets showing the cyan rectangles in (I4) and (L4) were enlarged as images in (J) for control (not subjected injury) and (M) for injured *NG2CreERT2;tdTomato* mice, respectively. Insets showing the dotted yellow rectangles in (J) and (M) were enlarged as images in (K1) to (K3) for control (not subjected injury) and (N1) to (N3) for injured *NG2CreERT2;tdTomato* mice, respectively. *NG2-tdTomato*$^+$ cells were embedded in the calcein label in the injury group (L2–L4, M, and N1–N3, arrowheads in N3), while *NG2-tdTomato*$^+$ cells were not clearly embedded but located beneath the mineralizing front in intact mice (I2–I4, J, and K1–K3). (**O**) A significant increase in the total number of embedded *NG2-tdTomato*$^+$ cells was observed in the injured condition, compared with cells not subjected to injury. Each bar represents the mean ± standard deviation of each experiment ($N = 3$ per group). A significant difference between columns (shown by solid line) is denoted by asterisks. The *P* value is shown (unpaired *t* test; parametric analysis). (**P and Q**) Odontoblast lineage cells (OLCs) were immunopositive for NG2 and ATF6a. Nuclei are shown in blue. (**R–T**) OLCs differentiated into osteocytes ([R], evaluated by Alizarin red staining), chondrocytes ([S], evaluated by Toluidine blue staining), and adipocytes ([T], evaluated by oil red O staining). (**U1–U4**) Alizarin red staining revealed that gene silencing of each *NG2* ([U2], green square in [U]), *ATF6a* ([U3], yellow square in [U]), and double gene silencing of both *NG2* and *ATF6a* ([U4], blue square in [U]) induced impairment of mineralization of OLCs compared with cells with *shControl* ([U1], orange square in [U]). (**V**) Significant decreases in the Alizarin red–stained area after mineralization induction in knocked-down cells by gene silencing with *shNG2* and/or *shATF6a* were observed compared with that in the control (*shControl*). Significant differences were analyzed by 1-way analysis of variance (ANOVA) with Tukey's post hoc test. Parentheses in (V) show the number of experiments conducted. Each bar in (V) represents the mean ± SD of each experiment. The *P* values are shown. (**W**) Representative scheme of this study shows that NG2$^+$ pericytes rapidly differentiate into functional odontoblasts after odontoblast death. Odontoblasts developmentally originate from glial cells (navy color cell lineages). After odontoblast death, pericytes in the cell-rich zone proliferate and differentiate into odontoblast progenitor cells and then odontoblasts (green color cell lineages). (**X**) Scheme shows Ca^{2+} signaling in NG2$^+$ Nestin$^+$ odontoblast progenitor cells. After odontoblast death by dentin/pulp injury, nuclear translocation of ATF6s is induced by the ER-stress response. The endoplasmic reticulum (ER)–stress response elicits Piezo1 upregulation to acquire mechanotransduction properties. The ER-stress response also activates the Na^+-Ca^{2+} exchanger (NCX) and plasma membrane Ca^{2+}-ATPase (PMCA) to extrude Ca^{2+} for reparative dentinogenesis. The ER is located at the distal side within the odontoblasts and closely physically interacts with Piezo1 channels via sarco/ER Ca^{2+}-ATPase (SERCA) pump. Through the Ca^{2+} signaling by ER physical interactions, it is highly possible that other molecules in addition to Piezo1 function in odontoblasts. Our group has revealed that there are functional couplings among Piezo1 channels and some transient receptor potential (TRP) channels via intracellular phospholipid metabolisms in odontoblasts (personal communications by T.O., R.K., and Y.S.). Thus, Ca^{2+} signaling at the subcellular membrane domain and intracellular organelle complicatedly modulates the odontoblast functions as sensory receptor cells and dentin-forming cells.

odontoblasts originating from NG2$^+$ pericytes. Injury models in the first molar of *NG2CreERT2;tdTomato* mice were established to observe the potential mineralization role of NG2$^+$ pericytes and their descendants (Fig. 5H). Calcein labeling in dentin–pulp borders in both control and injury model mice revealed that *NG2-tdTomato*$^+$ cells were located beneath the calcein-labeled mineralizing region in both conditions, and some *NG2-tdTomato*$^+$ cell populations were embedded in the mineralization front (Fig. 5I1–N3). The injured group had a higher number of embedded *NG2-tdTomato*$^+$ cells into calcein labeling than that of intact group (7-fold change) (Fig. 5O). These data suggest that NG2$^+$ pericytes are localized near CZ in steady-state condition in mouse molars, and NG2$^+$ pericytes drive dentin mineralization immediately after injury.

To evaluate the stem cell properties of NG2$^+$ pericytes, we demonstrated the differentiation assays of OLCs. The OLCs were immunopositive for NG2 and ATF6a antibodies (Fig. 5P, Q). OLCs also expressed mesenchymal stem cell (MSC) markers, CD73, CD90, and CD105 (Appendix Fig. 2G-I) and had the potential to differentiate into mesenchymal lineages such as osteocyte, chondrocyte, and adipocyte (Fig. 5R–T), confirming that NG2$^+$ ATF6a$^+$ OLCs matched with the definition of MSCs (Pittenger et al. 1999). To evaluate *NG2* and *ATF6a* regulation during mineralization, we performed gene silencing using *shRNA* and measured mineralization efficacies by Alizarin red staining. Genetic knockdown of *NG2* and/or *ATF6a* negatively regulated mineralization (Fig. 5U1-U4, V), suggesting that the specific odontoblast population participating in dentin mineralization has NG2$^+$ pericytes as their ancestor under the regulation of ATF6a (Fig. 5W, X).

Discussion

In the CZ adjacent to the OB, odontoblast progenitor cells were analyzed by Nestin reporter mice. Both Nestin$^+$ and Nestin$^-$ cells localized in the CZ proliferate and differentiate into odontoblast-like cells in response to odontoblastic depletion (Zhao et al. 2021). In the present study, we further showed that NG2$^+$ Nestin$^+$ cells regenerated in CZ after odontoblast depletion and expressed odontoblast markers. We also showed that NG2$^+$ cells are localized near CZ in steady-state condition and NG2$^+$ cells drive dentin mineralization after injury. These findings indicate that NG2$^+$ pericytes are a local cellular source of odontoblasts, as odontoblast progenitor cells that immediately differentiate into odontoblasts after severe dental pulp injury.

NG2 and Nestin are markers of MSCs (Méndez-Ferrer et al. 2010; Kunisaki et al. 2013; Ouchi et al. 2018). Recently, scRNA-seq revealed that Nestin is both an odontoblast progenitor cell marker and a pericyte marker (Gomes et al. 2022). Moreover, intrapulpal NG2$^+$ cells are not derived from glial

cells but from MSCs (Kaukua et al. 2014; Zhao et al. 2014). The results of this study support that the $NG2^+$ $Nestin^+$ pericytes are odontogenic mesenchymal progenitor cells localized in the periphery but not deep inside of the dental pulp and are capable of differentiating into functional odontoblasts.

ER stress is a state in which proteins with abnormal higher-order structures or proteins that have not undergone normal modification accumulate in the lumen of the ER. Such proteins are called "unfolded proteins" and are affected by various physiological stresses such as calcium depletion in the ER. Because ER stress damages cells, cells are equipped with a system to avoid this, called the ER-stress response (unfolded protein response; UPR). The accumulation of unfolded proteins in the ER is sensed by ER-stress sensor proteins (Ron and Walter 2007; Kim et al. 2008; Walter and Ron 2011).

Our present study showed that odontoblasts in steady-state condition expressed ATF6a, indicating that ATF6a in odontoblasts may physiologically sense the ER stress and function in the UPR process. After genetically somatic depletion of odontoblasts, $NG2^+$ cells in the CZ expressed Nestin and nuclear-translocated ATF6a. Thapsigargin, known as an ER-stress inducer, suppresses SERCA, resulting in the inhibition of Ca^{2+} uptake into the ER (Shaban et al. 2022). In the present study, thapsigargin induced nuclear translocation of ATF6a as the ER-stress response in OLCs. Our data revealed that thapsigargin increased $[Ca^{2+}]_i$. The increase was significantly inhibited by the application of the Piezo1 inhibitor. However, Piezo1 inhibitor did not inhibit the $[Ca^{2+}]_i$ increase by the activation of $P2Y_1R$. In addition, we could not observe nuclear translocation of ATF6a by activation of $P2Y_1R$. Thus, ER stress by the $[Ca^{2+}]_{ER}$ change via direct SERCA regulation augmented Piezo1-induced responses in odontoblast progenitor cells. PLC-coupled $P2Y_1R$ modulates the change in cell shape (Jin et al. 1998). The $[Ca^{2+}]_{ER}$ changes via $P2Y_1R$ activation may physiologically modulate cellular functions, such as cytoskeletal changes, through odontoblast development from the progenitor cells. ER is located between dentin and nuclei in odontoblasts (Liang et al. 2023). The presence of ER at the distal side within the odontoblasts may lead to odontoblasts effectively acting as sensory receptor cells and dentin-forming cells. Our data in the measurement of $[Ca^{2+}]_i$ showed the immediate response of Piezo1 inhibitor on the increase in thapsigargin-induced $[Ca^{2+}]_i$, suggesting that Piezo1 may directly interact with SERCA in odontoblasts at close range. Further in vivo studies to clarify how SERCA is inhibited in $NG2^+$ pericytes in CZ will lead to the development of regenerative therapy and preventive dentistry.

$NG2^+$ pericytes drove dentin mineralization after injury. When *ATF6a* and/or *NG2* were genetically downregulated by *shRNA*, mineralization was impaired. Several reports have suggested that Piezo1 negatively (Xu et al. 2024) or positively (Huang et al. 2024) regulates dentinogenesis. Under the process of dentinogenesis, reactionary dentinogenesis is driven by developmental and physiological intact odontoblasts, while reparative dentinogenesis is mediated by differentiated odontoblasts derived from dental pulp cells, especially as it was revealed that $NG2^+$ pericytes are the potential origin based on the present study. Thus, dentin regeneration is achieved through different origins. Based on previous reports and the present study, in the process of the formation of new reparative dentin by regenerated $Piezo1^+$ odontoblasts derived from $NG2^+$ pericytes, mineralization might be achieved by other drivers except for Piezo1. Although further study is needed, promotion of the acquisition of odontoblast characteristics originating from different types of cells will be a promising regenerative dentin therapy in the future.

In conclusion, the results of the present study showed that $NG2^+$ $Nestin^+$ cells beneath the odontoblasts are odontoblast progenitor cells. $NG2^+$ $Nestin^+$ cells that creep up from the CZ to OB are also involved in mechanosensitivity and dentin mineralization. ATF6a plays important roles in the differentiation of $NG2^+$ pericytes in the CZ into functional odontoblasts that act as sensory receptor cells and dentin-forming cells.

Author Contributions

T. Ouchi, M. Ando, R. Kurashima, M. Kimura, contributed to conception and design, data acquisition, analysis, and interpretation, drafted and critically revised the manuscript; N. Saito, A. Iwasaki, H. Sekiya, K. Nakajima, T. Hasegawa, T. Mizoguchi, Y. Shibukawa, contributed to conception and design, data interpretation, drafted and critically revised the manuscript. All authors declared no potential conflicts of interest with respect to the research, authorship, and publication of this article.

Declaration of Conflicting Interests

The authors declared no potential conflicts of interest with respect to the research, authorship, and/or publication of this article.

Funding

The authors disclosed receipt of the following financial support for the research, authorship, and/or publication of this article: This study was supported by the Japan Society for the Promotion of Science KAKENHI (grant Nos. 22K17025 [TO], 19K10117, 22K09972 [MK], 19H03833, 24K12953 [YS]), a Research Fund from the Nakatomi Foundation, a Research Fund from Nishiyama Dental Academy, the Tokyo Dental College Research Branding Project (Multidisciplinary Research Center for Jaw Disease [MRCJD]: Achieving Longevity and Sustainability by Comprehensive Reconstruction of Oral and Maxillofacial Functions), Tokyo Dental College Research Grant (Well-being Project), and Tokyo Dental College Dean's Encouragement Research Grant.

ORCID iD

T. Ouchi https://orcid.org/0000-0003-4258-2152

References

Aryal YP, Lee ES, Kim TY, Sung S, Kim JY, An SY, Jung JK, Ha JH, Suh JY, Yamamoto H, et al. 2020. Stage-specific expression patterns of ER stress-related molecules in mice molars: implications for tooth development. Gene Expr Patterns. 37:119130.

Charadram N, Farahani RM, Harty D, Rathsam C, Swain MV, Hunter N. 2012. Regulation of reactionary dentin formation by odontoblasts in response to polymicrobial invasion of dentin matrix. Bone. 50(1):265–275.

Feng J, Mantesso A, De Bari C, Nishiyama A, Sharpe PT. 2011. Dual origin of mesenchymal stem cells contributing to organ growth and repair. Proc Natl Acad Sci U S A. 108(16):6503–6508.

Fu Y, Ju Y, Zhao S. 2023. $Ca_v1.2$ regulated odontogenic differentiation of $NG2^+$ pericytes during pulp injury. Odontology. 111(1):57–67.

Goldberg M, Smith AJ. 2004. Cells and extracellular matrices of dentin and pulp: a biological basis for repair and tissue engineering. Crit Rev Oral Biol Med. 15(1):13–27.

Gomes NA, do Valle IB, Gleber-Netto FO, Silva TA, Oliveira HMC, de Oliveira RF, Ferreira LAQ, Castilho LS, Reis PHRG, Prazeres PHDM, et al. 2022. Nestin and NG2 transgenes reveal two populations of perivascular cells stimulated by photobiomodulation. J Cell Physiol. 237(4):2198–2210.

Huang P, Jiang RX, Wang F, Qiao WW, Ji YT, Meng LY, Bian Z. 2024. Piezo1 promotes odontoblast-mediated reactionary dentinogenesis via SEMA3A. J Dent Res. 103(9):889–898.

Jin J, Daniel JL, Kunapuli SP. 1998. Molecular basis for ADP-induced platelet activation. II. The P2Y1 receptor mediates ADP-induced intracellular calcium mobilization and shape change in platelets. J Biol Chem. 273(4):2030–2034.

Kaukua N, Shahidi MK, Konstantinidou C, Dyachuk V, Kaucka M, Furlan A, An Z, Wang L, Hultman I, Ahrlund-Richter L, et al. 2014. Glial origin of mesenchymal stem cells in a tooth model system. Nature. 513(7519):551–554.

Khatibi Shahidi M, Krivanek J, Kaukua N, Ernfors P, Hladik L, Kostal V, Masich S, Hampl A, Chubanov V, Gudermann T, et al. 2015. Three-dimensional imaging reveals new compartments and structural adaptations in odontoblasts. J Dent Res. 94(7):945–954.

Kim I, Xu W, Reed JC. 2008. Cell death and endoplasmic reticulum stress: disease relevance and therapeutic opportunities. Nat Rev Drug Discov. 7(12):1013–1030.

Kim JW, Choi H, Jeong BC, Oh SH, Hur SW, Lee BN, Kim SH, Nör JE, Koh JT, Hwang YC. 2014. Transcriptional factor ATF6 is involved in odontoblastic differentiation. J Dent Res. 93(5):483–489.

Kimura M, Mochizuki H, Satou R, Iwasaki M, Kokubu E, Kono K, Nomura S, Sakurai T, Kuroda H, Shibukawa Y. 2021. Plasma membrane Ca^{2+}-ATPase in rat and human odontoblasts mediates dentin mineralization. Biomolecules. 11(7):1010.

Kunisaki Y, Bruns I, Scheiermann C, Ahmed J, Pinho S, Zhang D, Mizoguchi T, Wei Q, Lucas D, Ito K, et al. 2013. Arteriolar niches maintain haematopoietic stem cell quiescence. Nature. 502(7473):637–643.

Li L, Wen Y, Jiang L, Zhu YQ. 2022. Endoplasmic reticulum stress response mediated by the PERK-eIF2α-ATF4 pathway is involved in odontoblastic differentiation of human dental pulp cells. Arch Oral Biol. 133:105312.

Liang T, Smith CE, Hu Y, Zhang H, Zhang C, Xu Q, Lu Y, Qi L, Hu JC, Simmer JP. 2023. Dentin defects caused by a $Dspp^{-1}$ frameshift mutation are associated with the activation of autophagy. Sci Rep. 13(1):6393.

Linde A, Lundgren T. 1995. From serum to the mineral phase. The role of the odontoblast in calcium transport and mineral formation. Int J Dev Biol. 39(1):213–222.

Lundgren T, Linde A. 1988. Na^+/Ca^{2+} antiports in membranes of rat incisor odontoblasts. J Oral Pathol. 17(9–10):560–563.

Lundgren T, Linde A. 1997. Voltage-gated calcium channels and nonvoltage-gated calcium uptake pathways in the rat incisor odontoblast plasma membrane. Calcif Tissue Int. 60(1):79–85.

Matsunaga M, Kimura M, Ouchi T, Nakamura T, Ohyama S, Ando M, Nomura S, Azuma T, Ichinohe T, Shibukawa Y. 2021. Mechanical stimulation-induced calcium signaling by Piezo1 channel activation in human odontoblast reduces dentin mineralization. Front Physiol. 12:704518.

Méndez-Ferrer S, Michurina TV, Ferraro F, Mazloom AR, Macarthur BD, Lira SA, Scadden DT, Ma'ayan A, Enikolopov GN, Frenette PS. 2010. Mesenchymal and haematopoietic stem cells form a unique bone marrow niche. Nature. 466(7308):829–834.

Nakatomi M, Quispe-Salcedo A, Sakaguchi M, Ida-Yonemochi H, Okano H, Ohshima H. 2018. Nestin expression is differently regulated between odontoblasts and the subodontoblastic layer in mice. Histochem Cell Biol. 149(4):383–391.

Neves VCM, Sharpe PT. 2018. Regulation of reactionary dentine formation. J Dent Res. 97(4):416–422.

Ohyama S, Ouchi T, Kimura M, Kurashima R, Yasumatsu K, Nishida D, Hitomi S, Ubaidus S, Kuroda H, Ito S, et al. 2022. Piezo1-pannexin-1-$P2X_3$ axis in odontoblasts and neurons mediates sensory transduction in dentinal sensitivity. Front Physiol. 13:891759.

Ouchi T, Morikawa S, Shibata S, Takahashi M, Yoshikawa M, Soma T, Miyashita H, Muraoka W, Kameyama K, Kawana H, et al. 2018. Recurrent spindle cell carcinoma shows features of mesenchymal stem cells. J Dent Res. 97(7):779–786.

Pittenger MF, Mackay AM, Beck SC, Jaiswal RK, Douglas R, Mosca JD, Moorman MA, Simonetti DW, Craig S, Marshak DR. 1999. Multilineage potential of adult human mesenchymal stem cells. Science. 284(5411):143–147.

Ron D, Walter P. 2007. Signal integration in the endoplasmic reticulum unfolded protein response. Nat Rev Mol Cell Biol. 8(7):519–529.

Sato M, Ogura K, Kimura M, Nishi K, Ando M, Tazaki M, Shibukawa Y. 2018. Activation of mechanosensitive transient receptor potential/Piezo channels in odontoblasts generates action potentials in cocultured isolectin B_4-negative medium-sized trigeminal ganglion neurons. J Endod. 44(6):984–991.e2.

Shaban MS, Mayr-Buro C, Meier-Soelch J, Albert BV, Schmitz ML, Ziebuhr J, Kracht M. 2022. Thapsigargin: key to new host-directed coronavirus antivirals? Trends Pharmacol Sci. 43(7):557–568.

Shibukawa Y, Sato M, Kimura M, Sobhan U, Shimada M, Nishiyama A, Kawaguchi A, Soya M, Kuroda H, Katakura A, et al. 2015. Odontoblasts as sensory receptors: transient receptor potential channels, pannexin-1, and ionotropic ATP receptors mediate intercellular odontoblast-neuron signal transduction. Pflugers Arch. 467(4):843–863.

Shibukawa Y, Suzuki T. 1997. Measurements of cytosolic free Ca^{2+} concentrations in odontoblasts. Bull Tokyo Dent Coll. 38(3):177–185.

Shibukawa Y, Suzuki T. 2003. Ca^{2+} signaling mediated by IP_3-dependent Ca^{2+} releasing and store-operated Ca^{2+} channels in rat odontoblasts. J Bone Miner Res. 18(1):30–38.

Tsumura M, Okumura R, Tatsuyama S, Ichikawa H, Muramatsu T, Matsuda T, Baba A, Suzuki K, Kajiya H, Sahara Y, et al. 2010. Ca^{2+} extrusion via Na^+-Ca^{2+} exchangers in rat odontoblasts. J Endod. 36(4):668–674.

Walter P, Ron D. 2011. The unfolded protein response: from stress pathway to homeostatic regulation. Science. 334(6059):1081–1086.

Xu X, Guo Y, Liu P, Zhang H, Wang Y, Li Z, Mei Y, Niu L, Liu R. 2024. Piezo mediates the mechanosensation and injury-repair of pulpo-dentinal complex. Int Dent J. 74(1):71–80.

Yang G, Ju Y, Liu S, Zhao S. 2019. Lipopolysaccharide upregulates the proliferation, migration, and odontoblastic differentiation of $NG2^+$ cells from human dental pulp in vitro. Cell Biol Int. 43(11):1276–1285.

Zhao H, Feng J, Seidel K, Shi S, Klein O, Sharpe P, Chai Y. 2014. Secretion of shh by a neurovascular bundle niche supports mesenchymal stem cell homeostasis in the adult mouse incisor. Cell Stem Cell. 14(2):160–173.

Zhao L, Ito S, Arai A, Udagawa N, Horibe K, Hara M, Nishida D, Hosoya A, Masuko R, Okabe K, et al. 2021. Odontoblast death drives cell-rich zone-derived dental tissue regeneration. Bone. 150:116010.